Makara Journal of Science

Volume 24
Issue 3 *September*

Article 5

9-18-2020

Sensitivity Enhancement of Silicon-on-Insulator Multipath Ring Resonator using Gold Nanodisk for Sensor Application

Gabriel Dicky
Lab-on-Chip Group, Biomedical Engineering Department, School of Electronics and Informatics, Bandung Institute of Technology, Bandung 40132, Indonesia, gabriel.dicky.a@students.itb.ac.id

Shidqie Taufiqurrahman
Lab-on-Chip Group, Biomedical Engineering Department, School of Electronics and Informatics, Bandung Institute of Technology, Bandung 40132, Indonesia

Topik Teguh Estu
Research Center for Electronics and Telecommunications (PPET), Indonesian Institute of Sciences (LIPI), Bandung 40135, Indonesia

Yusuf Nur Wijayanto
Research Center for Electronics and Telecommunications (PPET), Indonesian Institute of Sciences (LIPI), Bandung 40135, Indonesia

Robeth Viktoria Manurung
Research Center for Electronics and Telecommunications (PPET), Indonesian Institute of Sciences (LIPI), Bandung 40135, Indonesia

Recommended Citation

Dicky, Gabriel; Taufiqurrahman, Shidqie; Estu, Topik Teguh; Wijayanto, Yusuf Nur; Manurung, Robeth Viktoria; Mahmudin, Dadin; Anshori, Isa; and Daud, Pamungkas (2020) "Sensitivity Enhancement of Silicon-on-Insulator Multipath Ring Resonator using Gold Nanodisk for Sensor Application," *Makara Journal of Science*: Vol. 24 : Iss. 3 , Article 5.
DOI: 10.7454/mss.v24i3.1199
Available at: https://scholarhub.ui.ac.id/science/vol24/iss3/5

Sensitivity Enhancement of Silicon-on-Insulator Multipath Ring Resonator using Gold Nanodisk for Sensor Application

Authors

Gabriel Dicky, Shidqie Taufiqurrahman, Topik Teguh Estu, Yusuf Nur Wijayanto, Robeth Viktoria Manurung, Dadin Mahmudin, Isa Anshori, and Pamungkas Daud

Makara Journal of Science, 24/3 (2020), 172–178
doi: 10.7454/mss.v24i3.1199

Sensitivity Enhancement of Silicon-on-Insulator Multipath Ring Resonator using Gold Nanodisk for Sensor Application

Gabriel Dicky[1*], Shidqie Taufiqurrahman[1], Topik Teguh Estu[2], Yusuf Nur Wijayanto[2], Robeth Viktoria Manurung[2], Dadin Mahmudin[2], Isa Anshori[1], and Pamungkas Daud[2]

1. Lab-on-Chip Group, Biomedical Engineering Department, School of Electronics and Informatics, Institut Teknologi Bandung, Bandung 40132, Indonesia
2. Research Center for Electronics and Telecommunications (PPET), Indonesian Institute of Sciences (LIPI), Bandung 40135, Indonesia

[*]*E-mail: gabriel.dicky.a@students.itb.ac.id*

Received September 18, 2019 | Accepted April 20, 2020

Abstract

Currently, environmental degradation caused by heavy metals has become a serious concern of many countries. To monitor the concentration of heavy metals in the environment, an in-situ sensor that can measure in real time and has high quality, sensitivity, and flexibility is essential. We proposed a modified multipath ring resonator (MPRR) based on silicon-on-insulator technology with additional gold nanodisk (GND) on top of the ring to increase its sensitivity. To prove the effect of GND on the sensitivity of the modified MPRR, finite-difference time-domain simulations were conducted. Results showed that the average sensitivity of the modified MPRR was 675 nm/RIU, where RIU corresponds to the refractive index unit, higher than that of the unmodified MPRR (171 nm/RIU). Moreover, compared with the single ring structure, the proposed design had better sensitivity. We believe that our proposed approach for the modification of MPRR is suitable for application to optical sensor development.

Keywords: gold nanodisk, multipath ring resonator, sensitivity, sensor

Introduction

Aside from global warming, environmental problems have currently become a serious concern of society [1]. There are many pollutants in the environment, from nonbiodegradable plastics to dangerous substances, such as heavy metals [1,2]. Thus, daily monitoring of pollutant levels in the environment is critical to ensure that the concentration of these dangerous substances do not go beyond the upper limit. Traditionally, scientists need to obtain samples from the environment (e.g., rivers) and bring these samples to a laboratory. However, this method is considered outdated because sample collection requires time and cannot be done continuously 24 h a day [1]. These conditions led to the need for portable environmental sensors, that is, a compact yet powerful tool to monitor environmental parameters in real time, with good accuracy, high sensitivity, and full compatibility with standard microfabrication facilities for production [3,5].

Most of the commercial environmental sensors sold today are based on electronic signals (e.g., resistive and capacitive sensors), with the drawback of not having exceptional sensitivity [3]. Optical sensors have some advantages over their predecessors, such as high sensitivity, chemically inert, small, and lightweight, suitable for remote sensing, immunity to electromagnetic interference, wide dynamic range, and capable of monitoring a wide range of chemical and physical parameters [3].

Currently, various optical sensors, such as Mach–Zender interferometer [4], surface plasmon resonance [5,6], interferometers [7,8], resonant cavities [9–11], ring resonator [10,12], and microring resonator (MRR) one of the most promising optical sensors have been developed. Moreover, the MRR has different structures, such as single ring resonator (SRR) [13], serial cascaded microring resonator [14], parallel cascaded microring resonator [15], multi-coupled ring resonator [16], and multipath ring resonator (MPRR) [17,18]. The MPRR is arguably the most promising and suitable for sensor application [18,19]. In this study, we proposed a strategy to improve the sensitivity of the MPRR from design analysis to surface modification.

Multipath Ring Resonator. The MPRR has a pair of silicon waveguides and two ring resonators, as shown in The inner ring is circular, whereas the outer ring is elliptical. There are four ports, namely, input port (port 1),

output resonance (port 3), output antiresonance (port 2), and add port (port 4) [19]. Then, there is the cladding material that encloses the entire area around the ring resonators and silicon waveguides. The cladding material used depends on the analytes of interest [20,21]. How the sensor works is shown in Figure 1.

First, the light enters port 1. An optical phenomenon occurs within the waveguide called an evanescent field. Then, the evanescent field penetrates the cladding material, where the analyte is located. This phenomenon leads to the shifting of the light wave measured in port 3. Figure 2 shows an example of light wave transmittance measured in port 3 and the corresponding refractive index of the cladding material. The red line shows the wave transmitted when the refractive index of the cladding material is 1.00 (in this case, the material used is air). When the refractive index changes, for example, from 1.00 to 1.01, the light wave shifts, as shown by the green line. If the change of the refractive index is high, then the wave will shift far. The sensitivity of the MRR is calculated using the following equation:

$$S = \frac{\Delta\lambda}{\Delta n_{clad}} \tag{1}$$

where S refers to the sensitivity of the MRR, $\Delta\lambda$ represents the shifting of the wavelength, and Δn_{clad} corresponds to the change of the refractive index in the cladding material [21]. The unit of sensitivity is nm/RIU, where RIU corresponds to the refractive index unit.

Recent studies underlined the optimum configuration of MPRR with decent sensitivity and excellent free spectral range (FSR) and Q factor. However, sensitivity is compromised if the shifting of the light wave exceeds the FSR. This restricts the capability of the MPRR. To solve this problem, the MPRR can be modified by waveguide dispersion [22, 23]. Theoretically, this technique will broaden the FSR and consider the importance of adding a metal nanostructure to the structure of the MPRR for sensitivity enhancement. Waveguide dispersion can be accomplished by placing periodic arrays of gold nanodisks (GNDs) above the ring of the MPRR to produce a second-order Bragg grating, which can be expressed as follows:

$$m\lambda_B = 2n_{eff}\Lambda \tag{2}$$

where m = 2 (second order), λ_B refers to the Bragg wavelength, n_{eff} represents the refractive index of a particular mode at λ_B, and Λ corresponds to the period of the GNDs [22]. Because of these GNDs, interference emanates between the light that enters the ring resonator

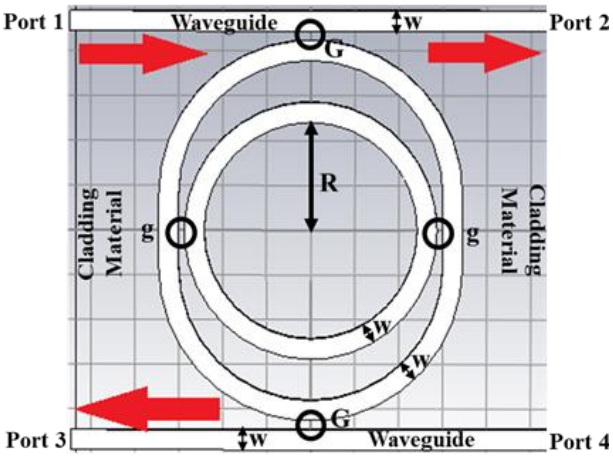

Figure 1. Schematic Diagram of the MPRR

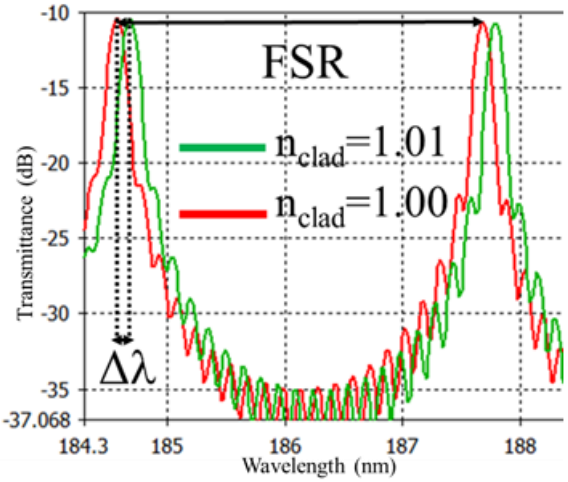

Figure 2. Illustration of the Wave Shifts Measured in Port 3 Caused by the Change of the Refractive Index

and the Bragg-reflected waves. This interference neutralizes most light wave resonances, which can be observed in the unmodified MRR [22]. However, this modification scheme that uses GNDs for the MRR has only been explored for the SRR structure. Thus, we investigated the use of this modification scheme for other structures and as the main strategy for sensitivity enhancement.

Design of the Modified Multipath Ring Resonator

In this study, we proposed a modified MPRR based on silicon-on-insulator technology targeted for sensor application. To prove the concept of waveguide dispersion by GNDs in this modified MPRR, 3D finite-difference time-domain (FDTD) simulations were conducted. Table 1 shows several parameters that were adjusted to determine the optimum sensitivity of the modified MPRR.

The optimum thickness of each GND has been optimized from that of a previous report, that is, 30 nm [22]. In this work, we investigated sensitivity enhancement by modifying the diameter of the GND structures and the number of GNDs on the surface of the MPRR. We started from the design of the unmodified MPRR, as shown in the schematic illustrated in Figure 1, that has the following parameters: ring resonator radius (R) = 3 mm, gap separation distance between the silicon waveguide and the ring resonator (G) = 200 nm, gap separation distance between the outer ring and the inner ring (g) = 130 nm, and waveguide width (w) = 450 nm. We set these parameters as the baseline for the modified MPRR. Figure 3(a) shows the schematic of the proposed design of the modified MPRR with GNDs arranged above the rings. The zoomed-in section of the top view of GNDs arranged above the ring, the cross section of the modified MPRR, and the dimensions of a GND are shown in Figures 3(b), 3(c), and 3(d), respectively.

To determine the optimum sensitivity of the modified MPRR, GNDs were configured through several trials. First, the radius of each GND was adjusted from 20 nm to 100 nm. Second, the distance between each GND was adjusted between 0.2 rad and 0.8 rad. We also experimented with GNDs placed above the inner ring only, above the outer ring only, and above both inner and outer rings. Referring to Figure 1, in these simulations, light entered the MPRR through port 1, and the output was measured in port 3. The transmittance measured in port 3 is similar to that shown in Figure 3, and from this information, the sensitivity was calculated. After the optimum parameter was determined, we compared the sensitivity between modified and unmodified MPRR and between an unmodified SRR structure without GNDs and a modified SRR structure.

Table 1. Parameters of the Modified MPRR

Parameter	Range	Unit
Radius of each GND	20–100	nm
Distance of each GND	0.2–0.8	rad
Placement of GNDs	Above the inner ring only, above the outer ring only, above both inner and outer rings	

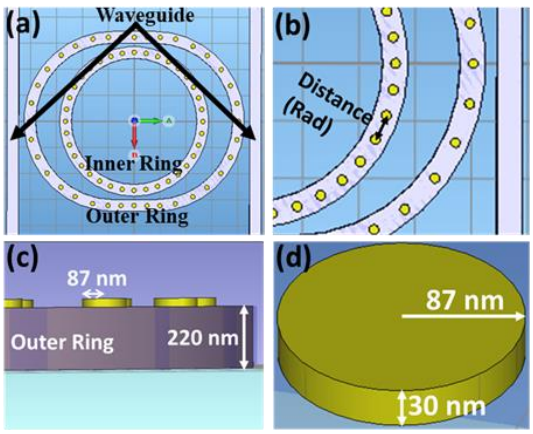

Figure 3. (a) Schematic of the Modified MPRR with GNDs, (b) Zoomed-in Section of the Modified MPRR, (c) Cross-sectional Diagram of the Modified MPRR, and (d) Dimensions of Each GND

Results and Discussion

For the first analysis, we adjusted the radius of the GNDs. Figure 4 illustrates the correlation between the radius of the GNDs and the sensitivity of the MPRR, with a constant value of n_{clad} (i.e., 1.33 RIU). We determined that the maximum sensitivity is reached when the radius of each GND is 87 nm, which is the same radius used in previous work on SRR [22]. The change of sensitivity due to the distance between each GND is shown in Figure 5. Figure 5 illustrates that the maximum sensitivity is reached when the distance between each GND is approximately 0.52 rad.

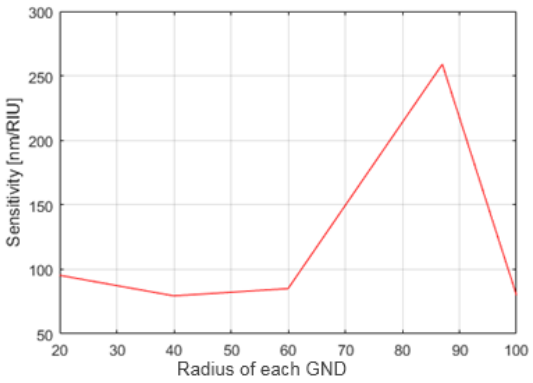

Figure 4. Sensitivity of the MPRR with GNDs of Different Radius, when n_{clad} is set to a Constant Value of 1.33 RIU

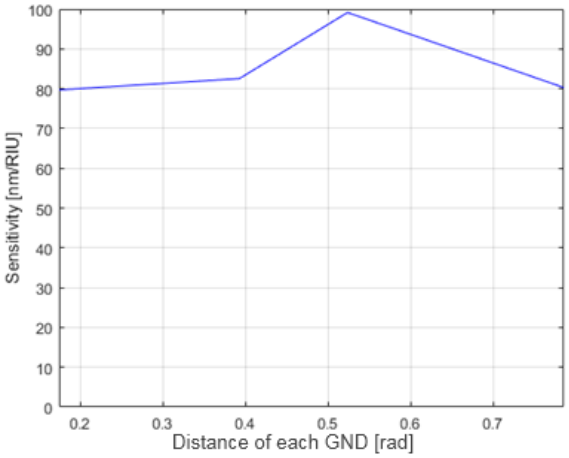

Figure 5. Correlation between the Distance of Each GND and the Sensitivity of the MPRR, when GNDs are Placed above the Inner Ring Only and n_{clad} is Set to a Constant Value of 1.33 RIU

Figure 6 illustrates how the modification of the GND structure affects the sensitivity of the MPRR by changing the wave shifts. In Figure 6(a), Δλ and the measured sensitivity are 0.854 nm and 85.43 nm/RIU, respectively. In Figure 6(b), Δλ and the measured sensitivity are 1.023 nm and 102.39 nm/RIU, respectively. In Figure 6(c), Δλ and the measured sensitivity are 1.025 nm and 102.59 nm/RIU, respectively. Figures 6(a), 6(b), and 6(c) show the effect of the change of the distance between each GND and its respective Δλ. The more the GNDs, the lesser the distance between each GND, thus creating a wider Δλ. Referring to Equation (1), if Δλ increases, then sensitivity also increases. The results confirmed that our modification scheme involving the change of the diameter of GNDs (Figure 4) and the distance between each GND (Figure 5) can be effectively used to determine the optimum configuration for the most sensitive designs.

The highest sensitivity is observed when each GND has a radius of 87 nm and there are 72 GNDs, with 36 GNDs on the inner ring and 36 GNDs on the outer ring. This configuration with the highest sensitivity is shown in the schematic illustrated in Figure 3(a), and the sensitivity comparison is presented in Figure 7. Then, we compared the changes of sensitivity when GNDs are placed above the inner ring only, above the outer ring only, and above both inner and outer rings. The results are shown in Table 2.

Then, the modified MPRR is compared with the unmodified MPRR. As presented in Figure 7, the modified MPRR exhibits a higher sensitivity than the unmodified MPRR. We also determined that the sensitivity of the MPRR increases when n_{clad} increases. For this simulation, we increased the value of n_{clad} from 1.00 to 3.30. The maximum sensitivity of the modified and unmodified MPRR is reached when the value of n_{clad} is 3.10. Inversely, the sensitivity of the MPRR decreases afterward with high cavity loss because Si has a refractive index of 3.47 [24]. The maximum sensitivity of the modified MPRR is 3,490.43 nm/RIU. By contrast, the maximum sensitivity of the unmodified MPRR is 1,042 nm/RIU. Additionally, when the refractive index is set to the minimum value of n_{clad} = 1.00 (the cladding material is air), the modified MPRR has slightly better sensitivity than the unmodified MPRR, with the sensitivity of 80.54 and 75.4 nm/RIU, respectively.

For the second analysis, the sensitivity of the modified MPRR is compared with a modified SRR presented in previous research [22]. The sensitivity comparison is shown in Table 3. Model A is the unmodified MPRR, Model B is the modified MPRR, Model C is the unmodified SRR (SRR without GNDs) [22], and Model D is the modified SRR (SRR with GNDs) [21]. These four structures are simulated under similar conditions at n_{clad} = 1.33 RIU (refers to water).

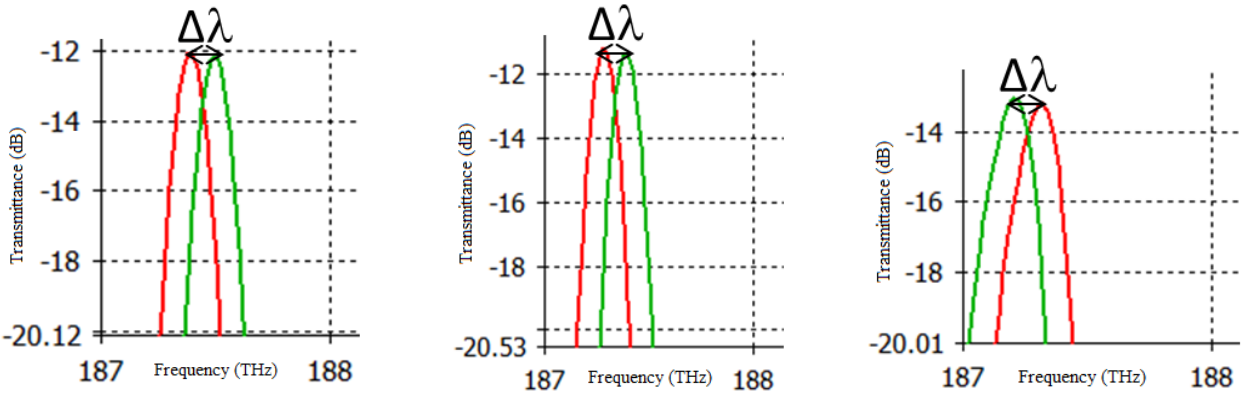

Figure 6. Illustration of the effect of GND on Sensitivity: (a) Wave Shifting from MPRR with 12 GNDs above the inner ring, Δλ = 0.854 nm, sensitivity = 85.43 nm/RIU; (b) wave shifting from MPRR with 18 GNDs above the inner ring, Δλ = 1.023 nm, sensitivity = 102.39 nm/RIU; (c) wave shifting from MPRR with 36 GNDs above the inner ring, Δλ = 1.025 nm, sensitivity = 102.59 nm/RIU

Table 2. Sensitivity Comparison of MPRR for Each Placement Option of GNDs, with n_{clad} = 1.33 RIU

Placement (number of GNDs)	Sensitivity
Above the inner ring only (36)	79.7 nm/RIU
Above the outer ring only (36)	95.71 nm/RIU
Above both inner and outer rings (72)	258.98 nm/RIU
Without GNDs (0)	98.28 nm/RIU

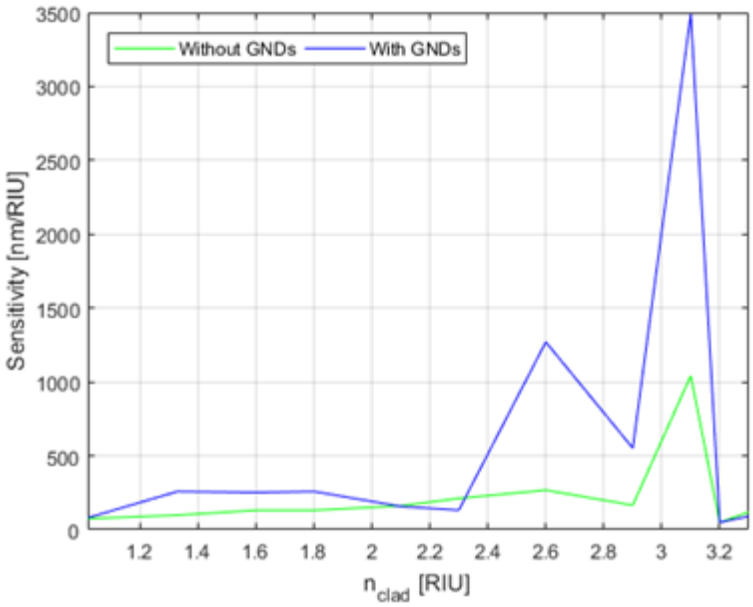

Figure 7. Sensitivity Comparison of the Unmodified MPRR (without GNDs) and Modified MPRR (with GNDs above Both Inner and Outer Rings) under Different n_{clad} Values while Δn_{clad} is set to a Constant Value of 0.01 RIU

Table 3. Sensitivity Comparison between Unmodified and Modified MPRR and SRR from [22]

	Model A	Model B	Model C	Model D
Sensitivity at n_{clad} = 1.33 ± 0.01	98.3 nm/RIU	258.98 nm/RIU	N/A	110 nm/RIU
Average sensitivity at the n_{clad} range of 1.00–2.60	171.64 nm/RIU	675.43 nm/RIU	70 nm/RIU	176 nm/RIU

The unmodified MPRR without GNDs has a sensitivity of 98.3 nm/RIU at n_{clad} = 1.33 RIU, which is slightly lower than that of the modified SRR with GNDs. Model A has an average sensitivity of 171.6 nm/RIU, which is slightly lower than that of Model D but more than twice that of Model C. This finding proves that the MPRR is superior to the SRR. Furthermore, when GNDs are added, the measured sensitivity at n_{clad} = 1.33 RIU and the average sensitivity increase drastically from 98.3 nm/RIU to 258.98 nm/RIU and from 171.64 nm/RIU to 675.43 nm/RIU, respectively. The average sensitivity here is calculated by taking the average of sensitivity within the n_{clad} range of 1.00–2.60 RIU. From the results shown in Table 3, we can conclude that the modified MPRR has the highest sensitivity compared with the unmodified MPRR, unmodified SRR, and modified SRR. However, the comparison is limited because this modified MPRR has only been explored for the single ring structure [21, 22].

Conclusion

In this study, a modified MPRR with GNDs was proposed and numerically verified. FDTD simulations were conducted to analyze the design and determine the optimum parameter for the modified MPRR. To determine the optimum sensitivity of the modified MPRR, 72 GNDs were required, separated by a distance of 0.52 rad. Every GND has a radius of 87 nm and a thickness of 30 nm. After modification with GNDs, the proposed MPRR reached the maximum sensitivity of 3,490 nm/RIU, and its average sensitivity was 675.43 nm/RIU. Compared with the unmodified MPRR, modified SRR, and unmodified SRR, the modified MPRR has the highest sensitivity when tested under the same conditions at n_{clad} = 1.33 RIU. On the basis of these results, we believe that the proposed MPRR design is highly applicable as a sensor with high sensitivity.

For further research, we propose that real experiments be conducted to prove these simulations. Given the limited resources, the modified MPRR design presented here has only been verified with modeling software. The same goes for the modified SRR that has only been verified by FDTD simulations.

Acknowledgements

This research was conducted as part of the research project entitled "Realization of light-based integrated sensor devices for detection of heavy metal from industrial waste as prevention of disaster in rivers and

lakes," through INSINAS research program 2019 from Ministry of Research, Technology and Higher Education of Republic of Indonesia.

References

[1] Bharagava, R.N., 2017. Environmental Pollutants and Their Bioremediation Approaches. Bioremediation. 1–22, http://dx.doi.org/10.1201/b22171-1.

[2] Förstner, U., Müller, G., 1973. Heavy metal accumulation in river sediments: A response to environmental pollution. Geoforum. 4(2): 53–61, http://dx.doi.org/10.1016/0016-7185(73)90006-7.

[3] Mcgrath, M.J., Scanaill, C.N., 2013. Environmental Monitoring for Health and Wellness. Sens. Techno. 249–282, http://dx.doi.org/10.1007/978-1-4302-6014-1_11.

[4] Densmore, A., Vachon, M., Xu, D.-X., Janz, S., Ma, R., Li, Y.-H., Lopinski, G., Delâge, A., Lapointe, J., Luebbert, C.C., Liu, Q.Y., Cheben, P., Schmid, J.H., 2009. Silicon photonic wire biosensor array for multiplexed real-time and label-free molecular detection. Opt. Lett. 34(23): 3598, http://dx.doi.org/10.1 364/ol.34.003598.

[5] Homola, J., 2003. Present and future of surface plasmon resonance biosensors. Anal. Bioanal. Chem. 377(3); 528–539, http://dx.doi.org/10.1007/s00216-003-2101-0.

[6] Debackere, P., Scheerlinck, S., Bienstman, P., Baets, R., 2007. Surface plasmon interferometer in silicon-on-insulator: novel concept for an integrated biosensor: Reply. Opt. Express. 15(21): 13651, http://dx.doi.org/10.1364/oe.15.013651.

[7] Ymeti, A., Greve, J., Lambeck, P.V., Wink, T., Hövell, V., Beumer, Wijn, R.R., Heideman, R.G., Subramaniam, V., Kanger, J.S., 2007. Fast, Ultrasensitive Virus Detection Using a Young Interferometer Sensor. Nano Lett. 7(2): 394–397, http://dx.doi.org/10.1021/nl062595n.

[8] Hradetzky, D., Mueller, C., Reinecke, H., 2006. Interferometric label-free biomolecular detection system. J. Opt. A Pure Appl. Opt. 8(7): S360–S364, http://dx.doi.org/10.1088/1464-4258/8/7/s11.

[9] Ksendzov, A., Lin, Y., 2005. Integrated optics ring-resonator sensors for protein detection. Opt. Lett. 30(24): 3344, http://dx.doi.org/10.1364/ol.30.003344.

[10] Yalcin, A., Popat, K., Aldridge, J., Desai, T., Hryniewicz, J., Chbouki, N., Little, B., King, O., Van, V., Chu, S., Gill, D., Anthes-Washburn, M., Unlu, M., Goldberg, B., 2006. Optical sensing of biomolecules using microring resonators. IEEE J. Sel. Top. Quant. Electron. 12(1): 148–155, http://dx.doi.org/10.1109/jstqe.2005.863003.

[11] Chao, C.-Y., Fung, W., Guo, L., 2006. Polymer microring resonators for biochemical sensing applications. IEEE J. Sel. Top. Quant. Electron. 12(1): 134–142, http://dx.doi.org/10.1109/jstqe.2005.862945.

[12] Passaro, V., Tullio, C., Troia, B., Notte, M., Giannoccaro, G., Leonardis, F., 2012. Recent Advances in Integrated Photonic Sensors. Sens. 12(11): 15558–15598, http://dx.doi.org/10.3390/ s121115558.

[13] Mulyanti, B., Pawinanto, R., Abdullah, A., Hasanah, L., Pantjawati, A., Hamidah, I., Nandiyanto, A., Zain, A.M., Menon, P., Shaari, S., 2018. Modeling of microring resonators for biochemical detection. Mater. Today Proc. 5(5): 13703–13710, http://dx.doi.org/10.1016/j.matpr.2018.02.008.

[14] Poon, J., Scheuer, J., Mookherjea, S., Paloczi, G.T., Huang, Y., Yariv, A., 2004. Matrix analysis of microring coupled-resonator optical waveguides. Opt. Express. 12(1): 90, http://dx.doi.org/10.1364/opex.1 2.000090.

[15] Melloni, A., 2001. Synthesis of a parallel-coupled ring-resonator filter. Opt. Lett. 26(12): 917, http://dx.doi.org/10.1364/ol.26.000917.

[16] Mahmudin, D., Estu, T.T., Daud, P., Armi, N., Wijayanto, Y., Wiranto, G., 2015. Environmental liquid waste sensors using polymer multi-coupled ring resonators. 2015 Int. Conference Smart Sens. Appl. http://dx.doi.org/10.1109/icssa.2015.7322 516.

[17] Hidayat, I., Toyota, Y., Torigoe, O., Wada, O., Koga, R., 2003. Multipath structure for FSR expansion in waveguide-based optical ring resonator. Electron. Lett. 39(4): 366, http://dx.doi.org/10.1049/el:20030276.

[18] Mahmudin, D., Estu, T.T., Daud, P., Hermida, I.D.P., Sugandi, G., Wijayanto, Y.N., Menon, P.S., Shaari, S., 2015. Sensitivity improvement of multipath optical ring resonators using silicon-on-insulator technology. 2015 IEEE Reg. Symp. Micro and Nanoelectron. http://dx.doi.org/10.1109/rsm.2015.7355021.

[19] Mahmudin, D., Rahman, A.N., Pristanto, E.J., Putranto, P., Desvasari, W., Setiawan, A., Darwis, F., Taufiqqurrachman, Sulistyaningsih, Hardiati, S., Kurniadi, D.P., Sugandi, G., Wijayanto, Y.N., Daud, P., 2019. Analysis of Multipath Optical Ring Resonator Structure for Single Side Band Microwave Photonic Filter Application. 2019 Int. Conference Electr. Electron. Inf. Eng. http://dx.doi.org/10.1109/iceeie47180.2019.8981434.

[20] Notte, M.L., Troia, B., Muciaccia, T., Campanella, C., Leonardis, F.D., Passaro, V., 2014. Recent Advances in Gas and Chemical Detection by Vernier Effect-Based Photonic Sensors. Sens. 14(3): 4831–4855, http://dx.doi.org/10.3390/s140304831.

[21] Steglich, P., Hülsemann, M., Dietzel, B., Mai, A., 2019. Optical Biosensors Based on Silicon-On-Insulator Ring Resonators: A Review. Mol. 24(3): 519, http://dx.doi.org/10.3390/molecules24030519.

[22] Urbonas, D., Balčytis, A., Gabalis, M., Vaškevičius, K., Naujokaitė, G., Juodkazis, S., Petruškevičius,

R., 2015. Ultra-wide free spectral range, enhanced sensitivity, and removed mode splitting SOI optical ring resonator with dispersive metal nanodisks. Opt Lett. 40(13): 2977, http://dx.doi.org/10.1364/ol.40.0029 77.

[23] Kuttge, M., Abajo F. Javier García De, Polman, A., 2010. Ultrasmall Mode Volume Plasmonic Nano-disk Resonators. Nano Lett. 10(5): 1537–1541, http://dx.doi.org/10.1021/nl902546r.

[24] Luan, E., Shoman, H., Ratner, D., Cheung, K., Chrostowski, L., 2018. Silicon Photonic Biosensors Using Label-Free Detection. Sens. 18(10): 3519, http://dx.doi.org/10.3390/s18103519.